Monthly Notices
of the
ROYAL ASTRONOMICAL SOCIETY

MNRAS **438,** 2307–2316 (2014)
Advance Access publication 2013 December 30

doi:10.1093/mnras/stt2345

Distribution and evolution of starspots on the RS CVn binary II Pegasi in 2004

Yue Xiang,[1,2,3] Sheng-hong Gu,[1,2★] A. Collier Cameron[4] and J. R. Barnes[5]

[1]*Yunnan Observatories, Chinese Academy of Sciences, Kunming 650011, China*
[2]*Key Laboratory for the Structure and Evolution of Celestial Objects, Chinese Academy of Sciences, Kunming 650011, China*
[3]*University of Chinese Academy of Sciences, Beijing 100049, China*
[4]*School of Physics and Astronomy, University of St Andrews, Fife KY16 9SS, UK*
[5]*Centre for Astrophysics Research, University of Hertfordshire, College Lane, Hatfield, Hertfordshire AL10 9AB, UK*

Accepted 2013 December 3. Received 2013 December 3; in original form 2013 July 15

ABSTRACT

We present Doppler images of RS CVn-type binary II Peg based on two data sets obtained in 2004 February and November. In order to improve signal-to-noise ratio and reliability, we apply least-squares deconvolution technique to calculate average profiles from 2032 photospheric absorption lines. Both of the resulting surface images show a wide latitude distribution of starspots. Most spots are concentrated at a high-latitude belt above 60° and a low-latitude belt near equator. The starspots evolved dramatically between two observing runs, which may indicate shorter time-scale evolution in this epoch, especially for low-latitude belt. There is no stable preferred active longitude that can be found in our images. We also find out a possible phenomenon that the intermediate-latitude spot migrated poleward and merged with the high-latitude spot to make it stronger, which may reveal a more complex behaviour of starspots on II Peg. A potential change of orbital ephemeris zero-point was detected. This may imply an orbital period change of II Peg like other active close binaries.

Key words: stars: activity – binaries: close – stars: imaging – stars: individual: II Peg – starspots.

1 INTRODUCTION

II Peg is a single-lined spectroscopic binary and classified as RS CVn-type by Rucinski (1977) and Vogt (1981). As one of the most active RS CVn binaries, II Peg shows large starspot coverage (Neff, O'Neal & Saar 1995), permanent strong Hα emission (Nations & Ramsey 1981; Frasca et al. 2008) and extreme X-ray flare (Osten et al. 2007). From long-term photometry, Rodonò et al. (2000) revealed that II Peg exhibits large photometric variability and cyclic starspot activity. Much weak differential rotations were also obtained by Rodonò et al. (2000), Siwak et al. (2010) and Roettenbacher et al. (2011) using photometric data.

Using high-resolution spectroscopic data, Berdyugina et al. (1998a) refined stellar parameters of II Peg. The result indicates that II Peg is composed of a K2IV subgiant primary and an unseen M-type dwarf secondary, with an orbital period of 6.72 d. The primary has a projected rotational velocity of $v \sin i = 22.6\,\mathrm{km\,s^{-1}}$ and an inclination of $i = 60°$. With radial velocity measurements, Berdyugina et al. (1998a) also derived a new improved orbital ephemeris,

$$T_{\mathrm{conj}} = \mathrm{HJD}\ 244\,9582.9268 + 6.724\,333E,$$

where the zero-point denotes the conjunction time when the primary is behind.

Because of the relatively high rotational speed, II Peg is suitable for Doppler imaging study. Doppler imaging technique can give much more details of surface starspot activity. Berdyugina et al. (1998b) derived nine surface images of II Peg, from spectroscopic data sets obtained during 1992–1996. In these images, the surface structure is usually dominated by two active longitudes separated by about 180°, and the spots are mainly located at 45°–75° latitude region. The active longitudes always show migration with a speed of $0\overset{\circ}{.}117\ \mathrm{d^{-1}}$. Switch between the strength of two active longitudes, called flip-flop phenomenon, was also found by them. Combined with six new images, Berdyugina et al. (1999) derived a period of 4.65 yr for flip-flop activity.

Recent Doppler imaging studies, however, do not support part of above results and show more complicated starspot activity on II Peg. The images obtained by Gu et al. (2003) and Lindborg et al. (2011) both show a dramatic change of main spot longitude, similar to flip-flop phenomenon, happened around the year 2001. The epoch is inconsistent with the prediction based on the flip-flop period derived by Berdyugina et al. (1999), which should be the year 2003. Further, Hackman et al. (2012) derived surface images from 2004 to 2010 and found no flip-flop phenomenon. In addition, the active longitude migration disappears in this duration. The distribution of starspots

★ E-mail: shenghonggu@ynao.ac.cn

becomes more chaotic since 2004. Hackman et al. (2012) supposed the reason of these changes is that II Peg gets in a low-activity level. By means of Zeeman–Doppler imaging, Kochukhov et al. (2013) obtained magnetic field distribution for the epoch 2004–2010, which supports the idea that II Peg is less active than before. Their result indicates that II Peg had maximum magnetic field at 2004, and it decreased after that, until 2009.

In summary, II Peg seems to get in a new state with very different starspot activity after the year 2003. In order to study the starspot activity of II Peg, especially short-term evolution, we have applied Doppler imaging technique to the spectroscopic data sets obtained in 2004 February and November. We shall describe the observation and data reduction in Section 2. The results will be given and discussed in Sections 3 and 4, respectively. In Section 5, we shall summarize this work.

2 OBSERVATION AND DATA REDUCTION

New observations of II Peg were performed on 2004 February 04–09 and November 21–29, using the Coudé echelle spectrograph (Zhao & Li 2001) mounted on the 2.16 m telescope at Xinglong station of National Astronomical Observatories, China. A 1024 × 1024 pixel TEK CCD detector was employed to record data. The spectral region was about 5500–9000 Å, and the resolution was $R = 37\,000$. The detailed observing log, including heliocentric Julian date of observation and exposure time, is listed in Table 1. Our exposure times correspond to 0.3–0.6 per cent of the orbital period of II Peg and are all short enough. The different exposure times do not affect our final image reconstructions.

Because the two-temperature model is employed in our image reconstruction, the spectra of two slowly rotating template stars, HR 222 (K2V) and HR 1703 (M0V), were also obtained to mimic local intensity profiles of photosphere and starspot of II Peg, respectively. Gu & Tan (2003) had shown that HR 222 of K2V type is a better template star than HR 495 of K2IV type for II Peg. Our template stars were observed by using the same instrument setup as II Peg.

Table 1. Observing log.

Date	HJD 245 0000+	Exp time (s)	S/N Input	S/N Output
2004 Feb.				
04	3039.9489	2400	170	2251
05	3040.9429	1800	190	2467
06	3041.9506	3600	203	2683
07	3042.9438	2400	153	2034
08	3043.9390	2400	241	3180
09	3044.9439	2400	169	2225
2004 Nov.				
21	3331.1464	3600	117	1781
22	3332.0816	3600	69	1050
22	3332.1238	3600	116	1770
23	3333.1002	3600	97	1482
25	3334.9996	3600	61	945
25	3335.0424	3600	65	1012
26	3336.0992	3600	83	1260
26	3336.1419	3600	88	1343
27	3337.1575	2400	125	1911
28	3338.1377	3600	64	986
29	3339.0998	3600	100	1527
29	3339.1425	3600	99	1518

The spectroscopic data were reduced with IRAF package in a standard way. The reduction procedure included image trimming, bias subtraction, flat-field dividing, scatter light subtraction, cosmic ray removal, wavelength calibration and continuum fitting. The wavelength calibration was carried out using comparison spectra of ThAr lamp for each night. However, due to the failure of ThAr lamp in the observing run of 2004 February, only one ThAr spectrum was obtained in the first night. We calibrated wavelength for all spectra of 2004 February with this unique ThAr spectrum, then corrected wavelength calibration error induced by instrumental shift in each night using telluric lines existed in the observed spectra. The detailed method and result will be described further in Section 2.1.

2.1 Least-squares deconvolution

Starspot signal is weak in the line profile. To improve signal-to-noise ratio (SNR) of the spectral line and obtain more accurate information of starspots, we used least-squares deconvolution (LSD) technique, which was developed by Donati et al. (1997), to calculate the average line profile from thousands of photospheric absorption lines, and improve SNR efficiently. The maximum SNR gain is the square root of the total number of used lines, but cannot be achieved in most cases (Donati et al. 1997).

For our data sets, velocity increment per pixel was set to 4.1 km s^{-1}, depending on the spectral resolution power. During the LSD calculation, the line list, including wavelength and depth, was obtained from Vienna Atomic Line Database (VALD; Kupka et al. 1999). The physical parameters of II Peg derived by Berdyugina et al. (1998a) were used to create the line list (see Table 2). Due to the 250 K interval of effective temperatures in VALD data base, we chose the effective temperature to be 4500 K, because the LSD calculation is not sensitive to the small variation of temperature (Barnes & Collier Cameron 2001). Lines in the regions around strong chromospheric emission lines (e.g. He I D_3, Na I Doublet, Hα, Ca II IRT) and telluric lines (e.g. H_2O, O_2) were removed from the list. The total number of used lines was 2032. As examples, we show the input spectra and the corresponding LSD profiles of 2004 February 6 and November 22 in Fig. 1. The input peak SNR as well as output SNR of each spectrum are also given in Table 1. The weighted centre of the deconvolved profile was at 6563 Å.

Besides, the spectra of the template stars (HR 222 and HR 1703) were also deconvolved with the same line list to produce local intensity profiles. In order to make lookup tables, we used a linear interpolation of limb-darkening coefficients given by Claret & Bloemen (2011) for *UBVRI* photometric bandpasses to obtain the limb-darkening coefficients at above centroidal wavelength. The results were 0.727 and 0.777 for photosphere and starspot, respectively. Then, we used 30 limb angles to make lookup tables for the photosphere and starspot of II Peg.

In spectroscopic observations, the internal instrumental shift will result in radial velocity error. As a result, the spurious spots will be reconstructed during Doppler imaging, or the imaging code even cannot converge (Collier Cameron 1999). In our case, radial

Table 2. Physical parameters of II Peg.

$T_{\rm eff}$ (K)	4600
$T_{\rm spot}$ (K)	3500
log g (cm s^{-2})	3.2
ξ_t (km s^{-1})	2.0
[Fe/H]	−0.4

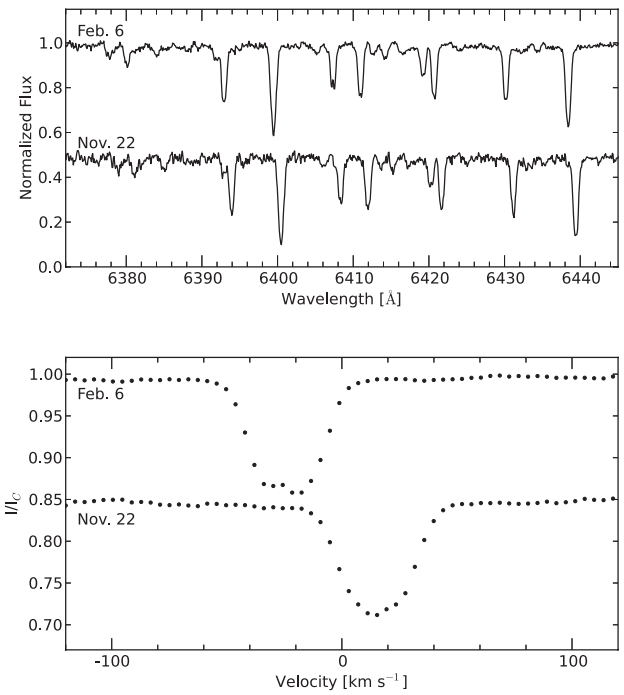

Figure 1. The upper panel shows parts of input spectra of II Peg obtained on 2004 February 6 and November 22, and SNR values are 203 and 69. The lower panel shows the corresponding output LSD profiles, and SNR values are 2683 and 1050.

velocity correction was performed with telluric lines using the method developed by Collier Cameron (1999). The telluric lines have negligible velocity and can be used as reference. Comparing with radial velocity standard stars, Donati et al. (2003) demonstrated that the precision of this method can be better than 0.1 km s^{-1}. At first, we performed LSD calculation with telluric line list for each spectrum, and used the first frame of each observing run as the master reference frame. Then, other frames were cross-correlated with the master one to derive the relative shifts. At last, the obtained shifts were removed from the deconvolved profiles. Because only one ThAr comparison spectrum was obtained in the first night of 2004 February run, and the observation of II Peg was made in the following six nights, we could expect that the same bias of radial velocity zero-point was introduced to all profiles of 2004 February. To determine the difference of zero-points between two observing runs, we performed cross-correlation calculation between two reference telluric frames, and got the relative shift of 5.33 km s^{-1}, which means a systematic wavelength shift of 0.117 Å at 6563 Å between two data sets.

3 DOPPLER IMAGING

3.1 System parameters

Doppler imaging is very sensitive to stellar parameters, and inaccurate parameters will make artefacts in reconstructed images (Collier Cameron & Unruh 1994). χ^2 minimization method can be used to fine-tune system parameters, such as radial velocity of mass centre (γ), $v \sin i$ and orbital ephemeris. This method is more suitable for the high SNR data and can eliminate the influence of starspot distortion in profile (Barnes et al. 2005). The detailed process was that we used Doppler imaging code DOTS (Doppler Tomography of Star; Collier Cameron 1992), for each parameter, to perform a fixed number of iterations to get a solution, and searched the best-fitting one. χ^2 minimization method can even be used to determine the parameters of double-lined contact binary, where stellar parameters are not independent (Barnes et al. 2004; Şenavcı et al. 2011). For the single-lined binary like II Peg, the situation is much simpler.

In practice, the initial values of parameters for II Peg were the ones derived by Berdyugina et al. (1998a). However, we found that the reduced χ^2 was too large when their orbital ephemeris zero-point (T_0) was used. Based on the fact that the variation of periods of close binaries is very small, we performed a grid search for T_0 with fixed radial velocity amplitude of primary (K_1) and orbital period (P). As shown in Fig. 2, we found significant difference to the original T_0 for both two data sets, and the results correspond to phase offsets of -0.00845 and -0.01291, which will be discussed further in Section 4.3. We also searched for radial velocity of mass centre and rotational velocity $v \sin i$, and the results are also shown in Fig. 2. The best-fitting system parameters are listed in Table 3. The errors of parameters were estimated according to how much variation makes $\Delta\chi^2 = 1$. Note that the rotational velocity $v \sin i$ was determined from the data set obtained in 2004 November, because of the better quality. The resulting value corresponds to $v \sin i = 22.0 \pm 0.9$ km s^{-1}. Besides, because of the different radial velocity zero-points, as mentioned in Section 2.1, γ was determined individually for two data sets. The difference between two values is consistent with the relative shift obtained in Section 2.1 within errors. This result indicates that the wavelength calibration correction was reliable.

3.2 Results

We used Doppler imaging code DOTS to perform maximum entropy image reconstruction. During the calculation, we used TEST statistic value of DOTS to estimate the number of iterations for convergence. When TEST value changes to increase steeply, the code begins to fit noise (Şenavcı et al. 2011). The final adopted number of iterations was 25 for our cases. Maximum entropy solutions as well as LSD profiles are plotted in Fig. 3, where we also display the contour representations of LSD profiles in the left-hand panels, and the orbital phase of each observation was calculated with the refined T_0. Resulting images of 2004 February and November are shown in Figs 4 and 5. Note that in our maps, longitude 0° is equal to the orbital phase 1 and longitude 360° is equal to the orbital phase 0.

In order to demonstrate the reliability of the image of 2004 February, we also made a test with the data set of 2004 November. The wavelength calibration for the data set was carried out with only one ThAr spectrum obtained on 2004 November 21, then we corrected radial velocity shift of each frame by telluric lines, as the same manner for 2004 February. The relative result is also plotted in Fig. 4 for comparison. We can see that there is no significant difference comparing with the image obtained above, especially for strong spots. Moreover, there is no new spurious feature in the test image, compared with the original one. This indicates that the image of 2004 February is reasonably reliable. The most obvious effect was the increasing of final reduced χ^2, which might mean relatively lower precision of wavelength calibration.

In the surface image of 2004 February, there is a weak high-latitude or polar spot with two connected starspot structures. One appendage is the feature of two connected spots with high strength at intermediate to low latitude, and the other appendage is weaker extended spots at low latitude (∼20°). Meanwhile, there are also isolated spots at very low latitude. One is the significant equatorial

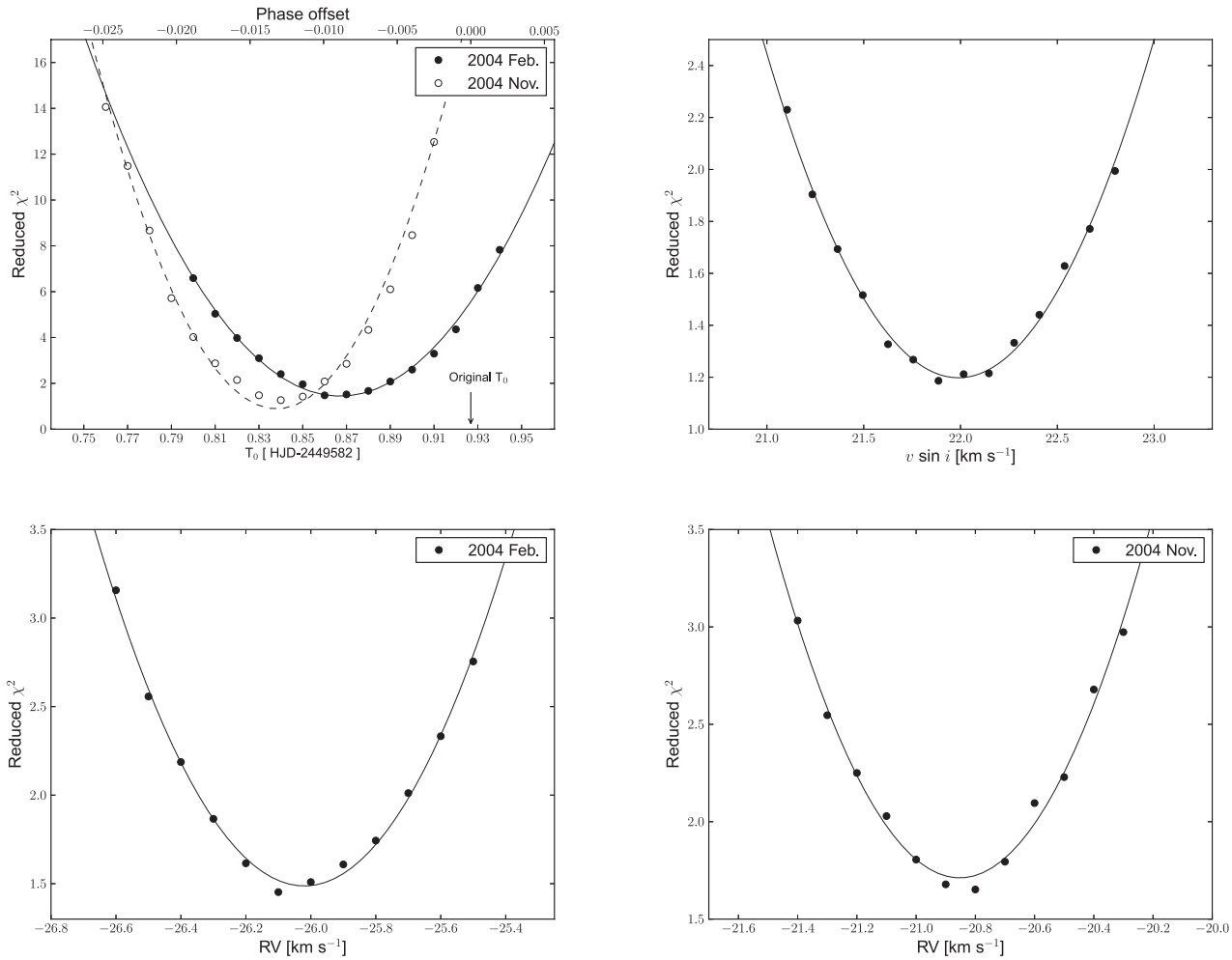

Figure 2. Resulting plots of searching for optimal parameters using χ^2 minimization. Top panels show the results of ephemeris and rotational velocity. The corresponding phase offset is also plotted on the upper x-axis. Bottom panels show the results of radial velocity of binary mass centre for 2004 February and November, respectively.

Table 3. Best-fitting system parameters.

Date	γ (km s^{-1})	$v \sin i$ (km s^{-1})	T_0 (HJD 240 0000)	K_1 [(a)] (km s^{-1})	Period[(a)] (d)	i[(a)] (deg)	M_2/M_1 [(a)]
Feb. 2004	-26.02 ± 0.46	22.0 ± 0.9	$495\,82.87 \pm 0.03$	38.66	6.724 333	60	0.5
Nov. 2004	-20.85 ± 0.48	22.0 ± 0.9	$495\,82.84 \pm 0.02$	38.66	6.724 333	60	0.5

[(a)] Adopted the values from Berdyugina et al. (1998a).

spot at longitude 210° and the other one is a low-latitude spot at longitude 140°. From the image of 2004 November, we can see an extended structure formed with two connected strong spots at high latitude (above 60° and reached the pole). The longitude range of the pattern is between about 60° and 230°. The high-latitude spots also have weak connected spot appendages extending to lower latitude. Besides, four individual low-latitude spots are located at longitude 140°, 170°, 300° and 350°. Their strength is much weaker than the high-latitude ones.

One should note that the spot near equator can be elongated vertically due to smearing of northern and southern features by Doppler imaging, especially for high-inclination stars (Collier Cameron & Unruh 1994). The effect can also make weak spurious features at very low latitude. So the discussion on the detailed shape and latitude of spots in equatorial belt should be taken carefully.

4 DISCUSSION

4.1 Latitude distribution of starspots

Rapid-rotating stars can exhibit high-latitude starspots, different from the Sun. In order to show the latitude distribution of starspots on II Peg, we plot the mean spot filling factor as a function of latitude in Fig. 6. As shown in the figure, most starspots of II Peg are concentrated at two active latitude belts in our new maps. One is higher than 60°and near the north pole and another is near equator.

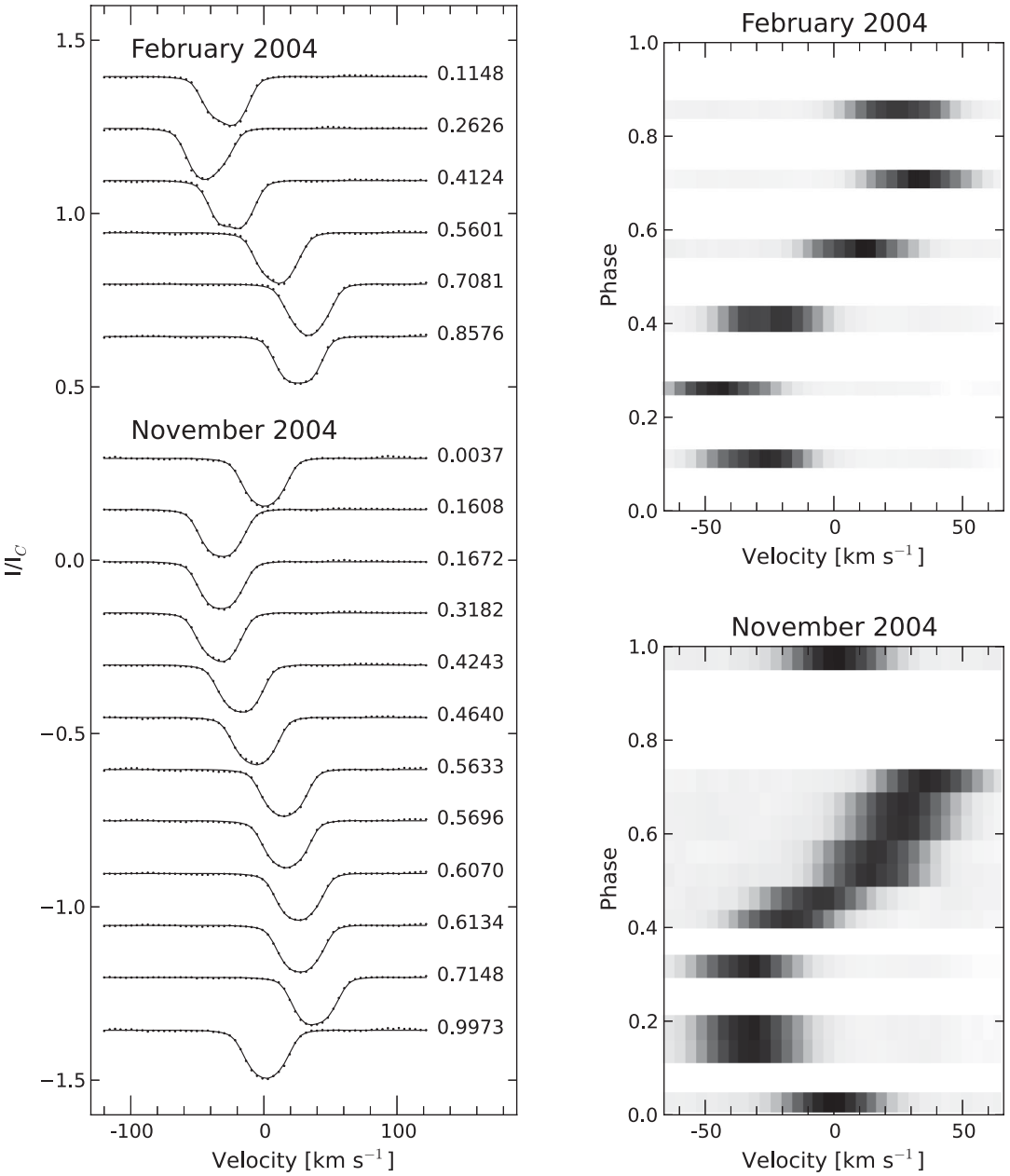

Figure 3. Right-hand panel shows LSD profiles (dots with error bars) and maximum entropy solutions (solid lines) for II Peg in 2004 February and November. The numbers beside profiles are the observing phases. Left-hand panels display the contour plot representations of LSD profiles.

In addition, some spots are also located at intermediate latitude. The latitude distribution of starspots is very wide. Especially, in 2004 February, the equatorial spot is very strong. This feature seems to come from the significant distortion in the profile at phase 0.4124 and the deformed shapes of profiles around this phase. So this spot is real, although the detailed shape and actual centre latitude is difficult to determine, as described in Section 3.2. In the temperature maps obtained by Lindborg et al. (2011), Hackman et al. (2012) and Kochukhov et al. (2013), there were also some spot features at much lower latitude and higher latitude. In contrast, images derived by Berdyugina et al. (1998b) revealed that the starspots always emerge in a narrow latitude belt between 45° and 75°.

We have also compared our result with other RS CVn stars. Three RS CVn-type binaries with K-type components and similar rotational speed, IN Vir (K2-3IV, $v_{\rm equ} = 27.7\,{\rm km\,s^{-1}}$; Strassmeier 1997), HU Vir (K0III-IV, $v_{\rm equ} = 27.6\,{\rm km\,s^{-1}}$; Strassmeier 1994) and IL Hya (K0III-IV, $v_{\rm equ} = 32.4\,{\rm km\,s^{-1}}$; Weber & Strassmeier 1998), were also reported to show similar distribution of starspots. They all have polar spots and IN Vir as well as IL Hya have equatorial cooler regions. These stars have relatively low rotational speeds among recent Doppler imaging studies. On the other hand, wide latitude distribution is a common phenomenon for stars with various physical parameters (Strassmeier 2009).

Schüssler et al. (1996) and Holzwarth (2004) have shown that starspots in high latitude can be explained by the influence of Coriolis force on magnetic flux tube in rapid-rotating young and evolved stars. The results of their simulations, however, can only support intermediate- to high-latitude spots, depending on the rotational

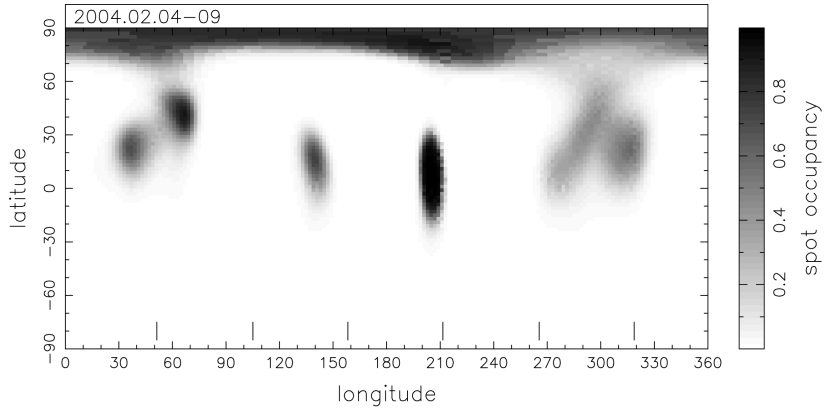

(a)

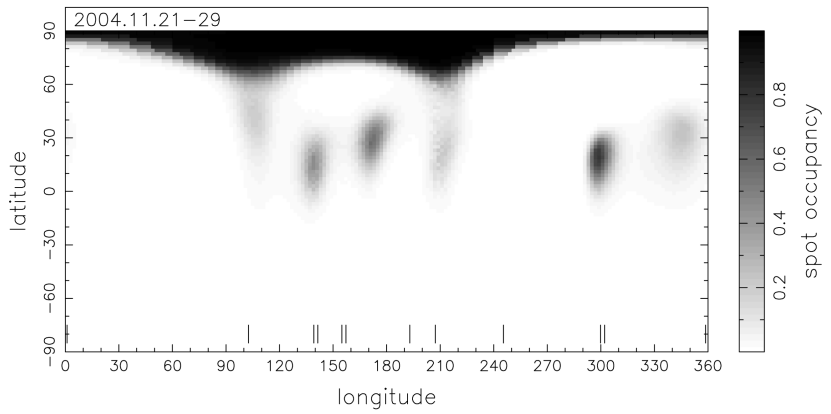

(b)

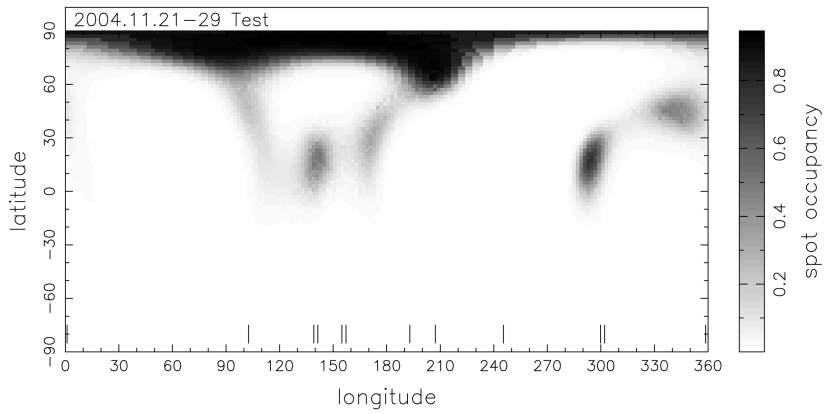

(c)

Figure 4. Mercator projection of reconstructed images of 2004 February (a), November (b) and the test for wavelength calibration correction (c). Observing phases are marked as ticks.

speed and depth of convection zone. Obviously, such a result is inconsistent with the starspot distribution on II Peg, and cannot explain too high- or too low-latitude starspots. Simulations made by Mackay et al. (2004) revealed that high-latitude features can also be produced by the effect of large meridional flows. Holzwarth, Mackay & Jardine (2006) show that the combined effect of Coriolis force and meridional circulation can influence the emergence of flux tube sufficiently and can produce polar features. In addition, low-latitude starspots may be formed by an equatorward drift of flux tubes before or after they emerged on the surface (Holzwarth 2004). The meridional flow rate of II Peg estimated by Weber (2007) is larger than 400 m s^{-1} and seems large enough. However, the detailed information about meridional circulation of II Peg is not clear so far. We may expect an important role of meridional circulation in latitude distribution for stars like II Peg.

4.2 Starspots evolution and migration

Our two new surface images are separated by nine months. Strength of starspots changed dramatically. As shown in Fig. 6, strong mean spot filling factor at low latitude decreased obviously, whereas the strength and range of high-latitude activity increased. On comparing

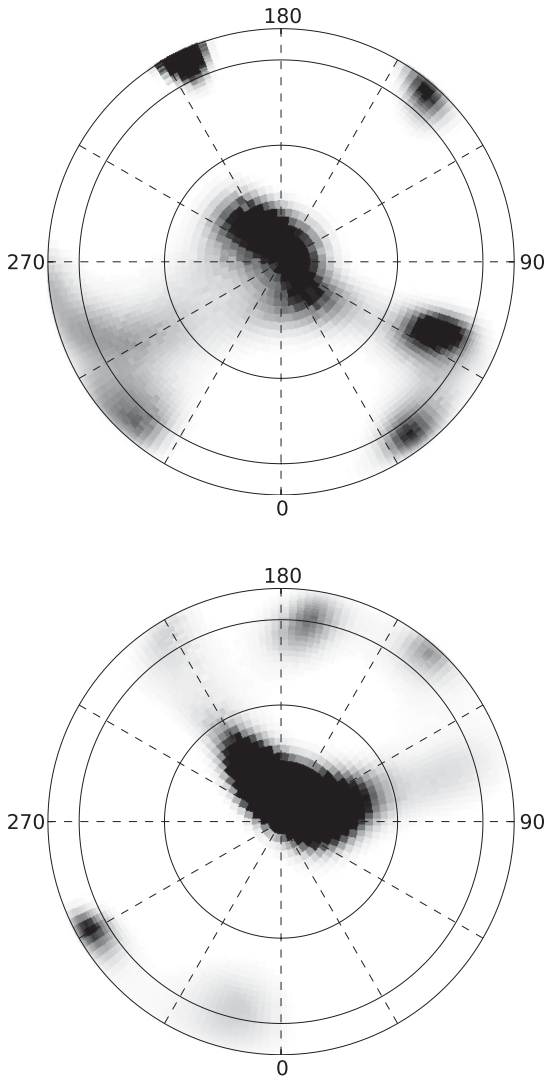

Figure 5. Polar projection of surface images for 2004 February and November.

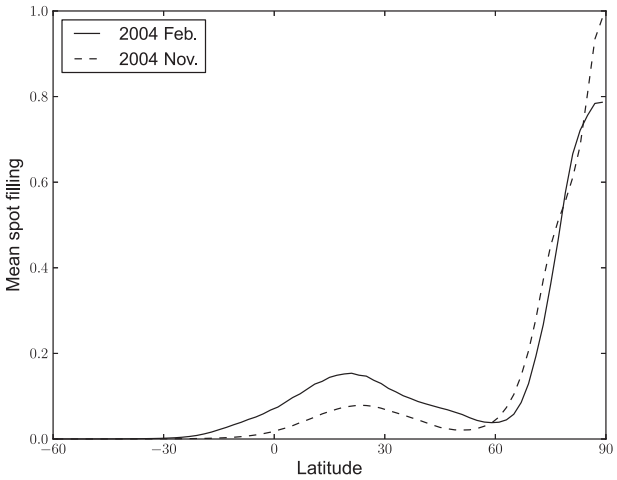

Figure 6. Mean spot filling factor as a function of latitude for 2004 February and November.

the two images, we can see that the strong equatorial spot on 2004 February seems to disappear in 2004 November and new spots appeared at low-latitude belt. Meanwhile, high-latitude spots still existed but the shape and strength changed significantly. However, in previous surface images, there was a stable starspot pattern for years (Gu et al. 2003; Lindborg et al. 2011). These may indicate that starspots have a shorter evolution time-scale in 2004 than before. The result is consistent with Hackman et al.'s (2011) result that spot evolution time-scale is months rather than years after the year 2004. In addition, low-latitude spots seem to have a much shorter lifetime, which is consistent with numerical simulation made by Işık, Schüssler & Solanki (2007). Kochukhov et al. (2013) also have compared two images in 2006 separated by three months to derive short-term evolution. As a result, temperature maps change little, and both have high-latitude extended spots and low-latitude spots, but magnetic field changes much. Considering this, we may infer that the lifetime of low-latitude spots is longer than three months but shorter than nine months.

Starspots on II Peg always emerged in two active longitudes separated by about 180° before 2004 (Berdyugina et al. 1998b; Gu et al. 2003). The active longitudes show migration and flip-flop phenomena. Holzwarth & Schüssler (2003) have shown that tidal force can affect the emergence of flux tube on close binaries, and produces preferred longitudes. In our images, however, there is no obvious preferred active longitude. The longitude distribution of starspots was random, and the spot patterns were not stable for nine months in the year 2004. The result is consistent with the ones of Hackman et al. (2012) and Kochukhov et al. (2013). We also infer that the vanishing of systemic migration and flip-flop behaviour was due to the rapid evolution of starspots.

From our surface maps, we derived starspot coverage of 0.0683 and 0.0414 in 2004 February and November, respectively. In order to show how spot coverage changes with time, we plot both the data from Hackman et al. (2012) and our results in Fig. 7. We can see that the spot coverage in February is slightly larger than the one in November, and both of them are significantly smaller than the ones before 2003. This indicates that spot coverage of II Peg had already decreased after 2004. This result supports that II Peg is in a low magnetic activity level, and we may infer that the spot activity of II Peg became weaker between 2003 and 2004. Starspot coverage on active stars can be also derived by measuring TiO band depths. II Peg had been studied with TiO band technique in the literatures, and spot filling factors between 26 and 64 per cent were derived in different seasons (Neff et al. 1995; O'Neal, Saar & Neff 1996; O'Neal, Neff & Saar 1998). We also investigated TiO bands to obtain spot coverage of II Peg, using the method developed by O'Neal et al. (1998). However, because 8860 Å TiO band was too close to the edge of the order during our observations, we can only

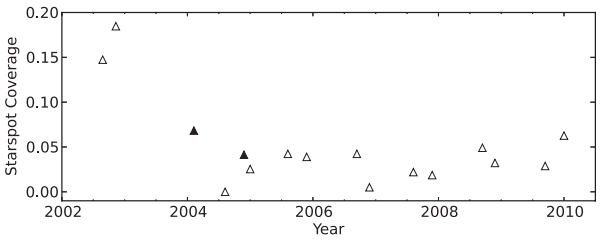

Figure 7. The starspot coverage as a function of time. Open triangles denote the results from Hackman et al. (2012). Solid ones represent ours.

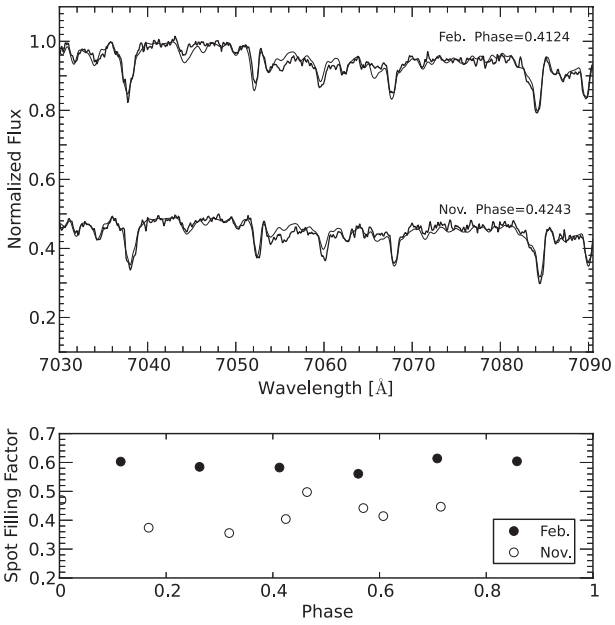

Figure 8. Upper panel shows sample spectra of 7055 Å TiO band and the STARMOD fit. Lower panel shows spot filling factors as a function of phase.

use 7055 Å band. After telluric features were removed using B-type star, we used STARMOD code (Barden 1985) to fit the II Peg spectra with photosphere and starspot standard stars, and obtained the best-fitting relative weights, which can be transferred to spot filling factors with equation 2 in O'Neal et al. (1998). R_λ, the ratio of continuum fluxes of starspot and photosphere, was obtained from the new grids of ATLAS9 fluxes (Castelli & Kurucz 2004). For the data set of November, we only select the higher SNR one if there are two spectra in the same night. Fig. 8 shows sample spectra of 7055 Å TiO band for February and November as well as the synthetic spectra. The spot filling factors were 0.56–0.62 in February and 0.36–0.50 in November. The spot coverage in February was larger than that in November. The changed trend of spot coverage is consistent with that obtained from Doppler imaging. However, the values are much larger than the ones derived by Doppler imaging, which was also found by Berdyugina et al. (1998b).

Our new images are quite compatible with two images obtained by both Hackman et al. (2012) and Kochukhov et al. (2013), which were based on the same data sets observed at epoches 2004 July–August and 2004 December to 2005 January. These four images compose an evolution sequence, from which some clues can be found for the starspot evolution in 2004. The intermediate-latitude spot around longitude 60° in 2004 February seems to be responsible for the formation of the strong high-latitude spot at longitude 60°–120° in November. We can find that a similar spot still exists at intermediate latitude and similar longitude in the images of 2004.6 derived by Hackman et al. (2012) and Kochukhov et al. (2013). So we suppose that this intermediate spot migrated poleward to high latitude and merged with the one there to become much stronger spot between 2004 February and November. In previous work, Gu et al. (2003) also found the possibility that low-latitude small spot migrated to higher location with the increase of strength. We can also suppose that poleward migration and mergence could induce the redistribution of starspot strength.

From consecutive observations, Vogt et al. (1999) and Strassmeier & Bartus (2000) found poleward propagation of starspot on the K-type subgiant component of RS CVn binary HR 1099. In their maps, low-latitude and intermediate-latitude starspots can slowly migrate to higher latitude and even merge with polar spot. Combined longitude and latitude migrations, the spot path shows clockwise spiral. Moss, Sokoloff & Lanza (2011) revealed that stars can exhibit various kinds of dynamo wave propagation (poleward, equatorward or both of them) within different physical quantities. The starspot behaviour we found is similar to theirs, but the path of starspot would be anticlockwise spiral. However, we should note that this can also be caused by starspot evolution of II Peg. The situation could be produced if the intermediate-latitude spot faded and new high-latitude spot emerged in the interval of nine months. The confirmation of such a behaviour requires more consecutive observations.

4.3 Period change

As mentioned in Section 3.1, using χ^2 minimization method, we found an obviously different T_0 from the one derived by Berdyugina et al. (1998a). We show how the orbital phase of the first conjunction (ϕ_0) changes with time in Fig. 9, based on the original ephemeris. It significantly deviates from zero, and seems to have a decreasing tendency. High SNR data are more sensitive to chosen system parameters, and Doppler imaging code cannot converge with much wrong parameters. The LSD profiles and the initial fit (unspotted profiles without iteration) using original T_0 for the data set of 2004 November are displayed in Fig. 10. As we can see, the misfit is significant and is more likely caused by a systemic phase offset, rather than the starspot distortion. So, it seems that the deviation was reliable within our data precision. We suppose that T_0 variation was induced by the accumulation of small orbital period changes, like many other active binaries.

Several active close binaries, including RS CVn, W UMa and Algol types, etc., have been found to show orbital period fluctuations (Lanza & Rodonò 1999). Most of them were detected by eclipse timing, because of the high precision. The period change can be induced by the third body in the system. However, the third component is not detected in most cases. Meanwhile, stellar magnetic activity could also induce orbital period changes with an order of $\Delta P/P \approx 10^{-5}$ for active close binary systems (Applegate 1992; Lanza 2005). As a similar RS CVn instance, Donati (1999) first

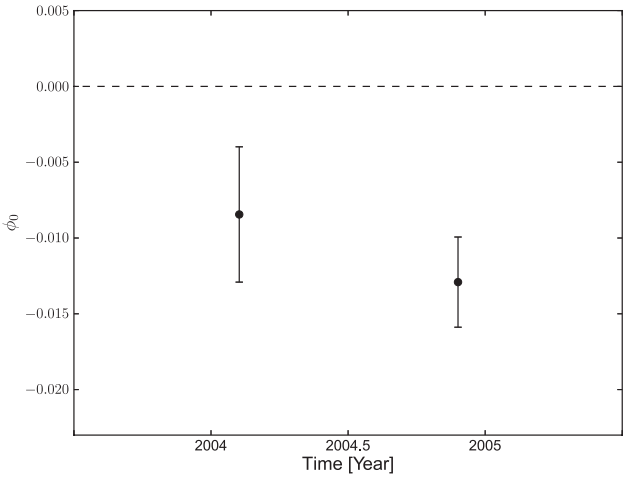

Figure 9. Orbital phase of conjunction time (ϕ_0) of each data set with error bar.

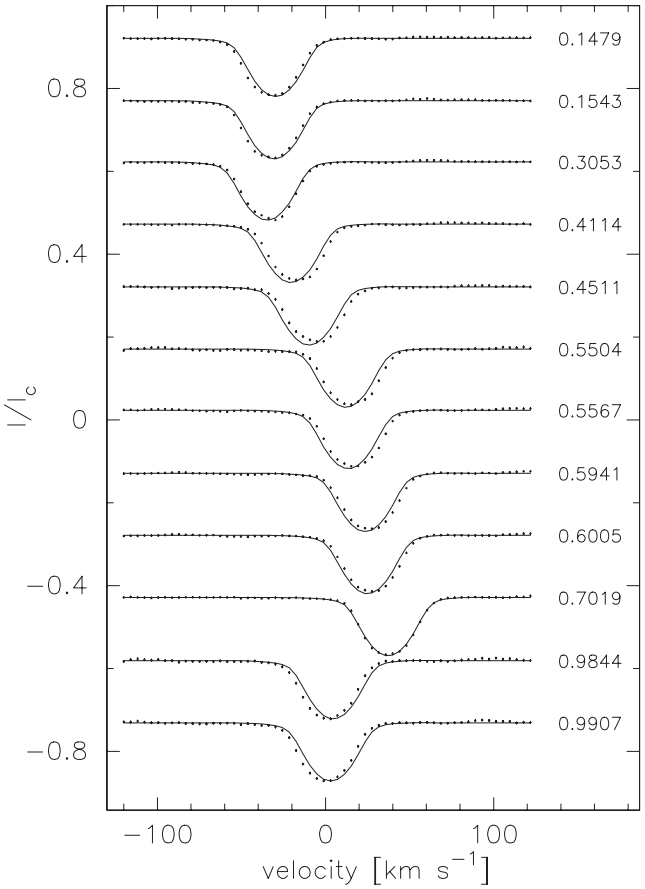

Figure 10. LSD profiles (dots) and unspotted profiles (lines) with the original T_0.

detected the fluctuation of orbital period of HR 1099 by using high-SNR LSD profiles. Furthermore, from long-term observations, Muneer et al. (2010) derived periods of period change and magnetic activity of HR 1099, and found that there is a correlation between orbital period modulation and starspot activity. II Peg is a very active close binary, and we suppose the orbital period change detected here was also induced by the similar mechanism. The amplitude of phase offset, however, is much smaller than others, perhaps because of the relatively longer orbital period, similar to the situation of UX Ari discussed by Muneer et al. (2010). For II Peg, long-term precise spectroscopic observations are required for further investigation on its period change. The study on period modulation may be helpful to understand the magnetic activity level of II Peg and even the interaction between the primary and unseen secondary.

5 CONCLUSION

We have presented two Doppler images of II Peg from data sets obtained in 2004 February and November. Based on our new surface images and relative analysis, we summarize our results as follows.

(1) In new images, starspots of II Peg were widely distributed in latitudes. Most spots were concentrated at a high-latitude belt and an equatorial belt.

(2) The evolution time-scale of starspots became much shorter than before, and no stable preferred active longitude was found in 2004. This may be responsible for the vanishing of spot migration found in previous works.

(3) We found a possible behaviour that the intermediate-latitude spot migrated to high latitude and merged with the one there to become much stronger. This fact may indicate a more complex migration and evolution of starspots on II Peg, similar to the well-studied RS CVn binary HR 1099.

(4) A significant phase offset was detected, which might indicate a possible orbital period change of II Peg.

Our results suggest that more consecutive observations with shorter intervals are required for further study on complicated starspot behaviour of II Peg, which is insufficient for II Peg so far.

ACKNOWLEDGEMENTS

We would like to thank Professor Jian-yan Wei and Professor Xiao-jun Jiang for the allocation of observing time at Xinglong 2.16 m telescope. We are very grateful to the anonymous referee for his or her valuable comments and suggestions, which significantly improved our manuscript. This work is supported by National Natural Science Foundation of China through grants Nos. 10373023, 10773027 and 11333006, Chinese Academy of Sciences through project KJCX2-YW-T24.

REFERENCES

Applegate J. H., 1992, ApJ, 385, 621
Barden S. C., 1985, ApJ, 295, 162
Barnes J. R., Collier Cameron A., 2001, MNRAS, 326, 950
Barnes J. R., Lister T. A., Hilditch R. W., Collier Cameron A., 2004, MNRAS, 348, 1321
Barnes J. R., Collier Cameron A., Lister T. A., Pointer G. R., Still M. D., 2005, MNRAS, 356, 1501
Berdyugina S. V., Jankov S., Ilyin I., Tuominen I., Fekel F. C., 1998a, A&A, 334, 863
Berdyugina S. V., Berdyugin A. V., Ilyin I., Tuominen I., 1998b, A&A, 340, 437
Berdyugina S. V., Berdyugin A. V., Ilyin I., Tuominen I., 1999, A&A, 350, 626
Castelli F., Kurucz R. L., 2003, in Piskunov N., Weiss W. W., Gray D. F., eds, Proc. IAU Symp. 210, Modelling of Stellar Atmospheres. Astron. Soc. Pac., San Francisco, p. A20
Claret A., Bloemen S., 2011, A&A, 529, A75
Collier Cameron A., 1992, in Byrne P., Mullan D., eds, Lecture Notes in Physics, Vol. 397, Surface Inhomogeneities on Late-Type Stars. Springer-Verlag, Berlin, p. 33
Collier Cameron A., 1999, in Hearnshaw J. B., Scarfe C. D., eds, ASP Conf. Ser. Vol. 185, Precise Stellar Radial Velocity. Astron. Soc. Pac., San Francisco, p. 233
Collier Cameron A., Unruh Y. C., 1994, MNRAS, 269, 814
Donati J.-F., 1999, MNRAS, 302, 457
Donati J.-F., Semel M., Carter B. D., Rees D. E., Collier Cameron A., 1997, MNRAS, 291, 658
Donati J.-F. et al., 2003, MNRAS, 345, 1145
Frasca A., Biazzo K., Taş G., Evren S., Lanzafame A. C., 2008, A&A, 479, 557
Gu S.-H., Tan H.-S., 2003, in Brown A., Harper G. M., Ayres T. R., eds, Proc. 12th Cambridge Workshop on Cool Stars, Stellar Systems, and the Sun, The Future of Cool-Star Astrophysics. Univ. of Colorado, Boulder, p. 986
Gu S.-H., Tan H.-S., Wang X.-B., Shan H.-G., 2003, A&A, 405, 763
Hackman T. et al., 2011, Astron. Nachr., 332, 859
Hackman T., Mantere M. J., Lindborg M., Ilyin I., Kochukhov O., Piskunov N., Tuominen I., 2012, A&A, 538, A126
Holzwarth V., 2004, Astron. Nachr., 325, 408
Holzwarth V., Schüssler M., 2003, A&A, 405, 303

Holzwarth V., Mackay D. H., Jardine M., 2006, MNRAS, 369, 1703
Işık E., Schüssler M., Solanki S. K., 2007, A&A, 464, 1049
Kochukhov O., Mantere M. J., Hackman T., Ilyin I., 2013, A&A, 550, A84
Kupka F., Piskunov N., Ryabchikova T. A., Stempels H. C., Weiss W. W., 1999, A&AS, 138, 119
Lanza A. F., 2005, MNRAS, 364, 238
Lanza A. F., Rodonò M., 1999, A&A, 349, 887
Lindborg M., Korpi M. J., Hackman T., Tuominen I., Ilyin I., Piskunov N., 2011, A&A, 526, A44
Mackay D. H., Jardine M., Collier Cameron A., Donati J.-F., Hussain G. A. J., 2004, MNRAS, 354, 737
Moss D., Sokoloff D., Lanza A. F., 2011, A&A, 531, A43
Muneer S., Jayakumar K., Rosario M. J., Raveendran A. V., Mekkaden M. V., 2010, A&A, 521, A36
Nations H. L., Ramsey L. W., 1981, AJ, 86, 433
Neff J. E., O'Neal D., Saar S. H., 1995, ApJ, 452, 879
O'Neal D., Saar S. H., Neff J. E., 1996, ApJ, 463, 766
O'Neal D., Neff J. E., Saar S. H., 1998, ApJ, 507, 919
Osten R. A., Drake S., Tueller J., Cummings J., Perri M., Moretti A., Covino S., 2007, ApJ, 654, 1052
Rodonò M., Messina S., Lanza A. F., Cutispoto G., Teriaca L., 2000, A&A, 358, 624
Roettenbacher R. M., Harmon R. O., Vutisalchavakul N., Henry G. W., 2011, AJ, 141, 138
Rucinski S. M., 1977, PASP, 89, 280
Schüssler M., Caligari P., Ferriz-Mas A., Solanki S. K., Stix M., 1996, A&A, 314, 503
Şenavcı H. V., Hussain G. A. J., O'Neal D., Barnes J. R., 2011, A&A, 529, A11
Siwak M., Rucinski S. M., Matthews J. M., Kuschnig R., Guenther D. B., Moffat A. F. J., Sasselov D., Weiss W. W., 2010, MNRAS, 408, 314
Strassmeier K. G., 1994, A&A, 281, 395
Strassmeier K. G., 1997, A&A, 319, 535
Strassmeier K. G., 2009, A&AR, 17, 251
Strassmeier K. G., Bartus J., 2000, A&A, 354, 537
Vogt S. S., 1981, ApJ, 247, 975
Vogt S. S., Hatzes A. P., Misch A. A., Kürster M., 1999, ApJS, 121, 547
Weber M., 2007, Astron. Nachr., 328, 1075
Weber M., Strassmeier K. G., 1998, A&A, 330, 1029
Zhao G., Li H.-B., 2001, Chin. J. Astron. Astrophys., 1, 555

This paper has been typeset from a TEX/LATEX file prepared by the author.